EUROPEAN ORGANIZATION FOR NUCLEAR RESEARCH
CERN - AB DIVISION

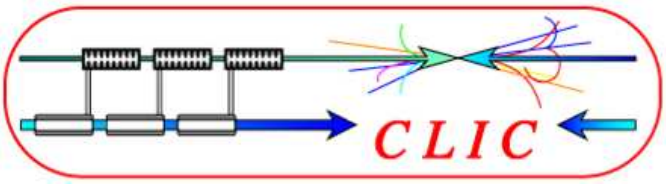

CLIC-Note-735

Optimizing the CLIC Beam Delivery System

R. Tomás and M. Jørgensen

Abstract

The optimization of the new CLIC Final Focus System (FFS) with L^*=3.5m is presented for a collection of CLIC beam parameters. The final performance is computed for the full Beam Delivery System including the new diagnostics section. A comparison to previous designs is also presented.

Geneva, Switzerland
March 13, 2008

1 Introduction

Since 2005 the CLIC Beam Delivery System (BDS) and, more in particular, the FFS are undergoing different optimizations to maximize their performance, namely total and peak luminosities. The starting point of these optimizations is based on the minimization of the non-linear aberrations of the FFS, presented in [1]. Basically non-linear elements are used to minimize the horizontal and vertical IP spot sizes using the Simplex algorithm [2]. In this paper we refer to *sextupole optimization* when only lattice sextupoles are considered to minimize the IP spot sizes. By *full non-linear optimization* we imply that extra non-linear elements like octupoles and decapoles are introduced in the beam line to better cancel high order aberrations.

Later this procedure was extended to optimize the lattice dispersion as well [3, 4]. Lowering dispersion reduces the emittance growth due to synchrotron radiation but enlarges chromatic aberrations, therefore there must be an optimum dispersion for which the IP spot size is minimum.

All these optimizations are carried out using MAPCLASS [5], which is a Python code that reads map coefficients and twiss parameters from MADX-PTC [6, 7] output to compute beam sizes at the IP. MAPCLASS has an implementation of the Simplex algorithm to minimize IP beam sizes. It has also been used in the totally different environment of the LHC IR upgrade studies [8]. Minimum beam sizes at the IP do not guarrantee maximum peak luminosity. The last step of the optimization involves computing the luminsotiy using the GUINEA-PIG code [9], always taking into account radiation effects.

From the point of view of optics and cost, shorter focusing systems are preferred since, for a given β^*, beta functions are smaller and the tunnel is also shorter. However detector integration becomes more difficult for shorter L*. We have considered 3 cases with L* having the values: 4.3m, 3.5m and 2.8m. The longest one with 4.3m was the original FFS. Fig. 1 shows the total luminosity versus the FFS length for the different stages of the optimization, namely: sextupole optimization, full non-linear optimization and dispersion optimization. The initial design in 2005 is labeled as "Nominal FFS" on the plot. It is the longest FFS with an L*=4.3m. A shorter L* implies lower beta-function and lower chromatic aberrations. The first shortening attempt at L*=2.8m (360m FFS length) showed a clear gain in luminosity without having applied all the steps of the optimization. However this L* could pose problems in the integration of the detector. It was decided to set L* to 3.5m ($\approx$460m FFS length) to avoid any possible conflict with the detector. In the meantime the CLIC beam parameters have changed. The bunch length and the normalized vertical emittance have increased from 35μm to 44μm and from 10nm to 20nm, respectively. The new lattice with L*=3.5m and the new set of CLIC beam parameters require a thorough re-optimization. In the following sections the optimizations for this and other interesting sets of parameters are presented.

2 Optimization of the L*=3.5m FFS

To illustrate the non-linear optimization procedure, described above, Fig. 2(a) shows the luminosity in the 1% energy peak at all stages of the optimization. A strong dependence of the peak luminosity on the horizontal beam size is observed. Figure 2(b) shows a zoom of the clear borderline that encloses the achievable beam sizes. At this level reducing the horizontal beam size implies increasing the vertical size and vice-versa. The maximum luminosity can be found in the lower right corner of Fig. 2(b).

Lowering the dispersion implies less synchrotron radiation in the FFS while it requires stronger non-linear elements to cancel the chromatic aberrations. To find the optimum dispersion along the FFS various optics are prepared having different dispersion levels. The non-linear optimization is ran for the different optics. Lastly the luminosities of these options are computed to select the best. Figure 3(a) and (c) show the IP beam sizes with and without radiation versus dispersion reduction for $\epsilon_y = 10$nm and

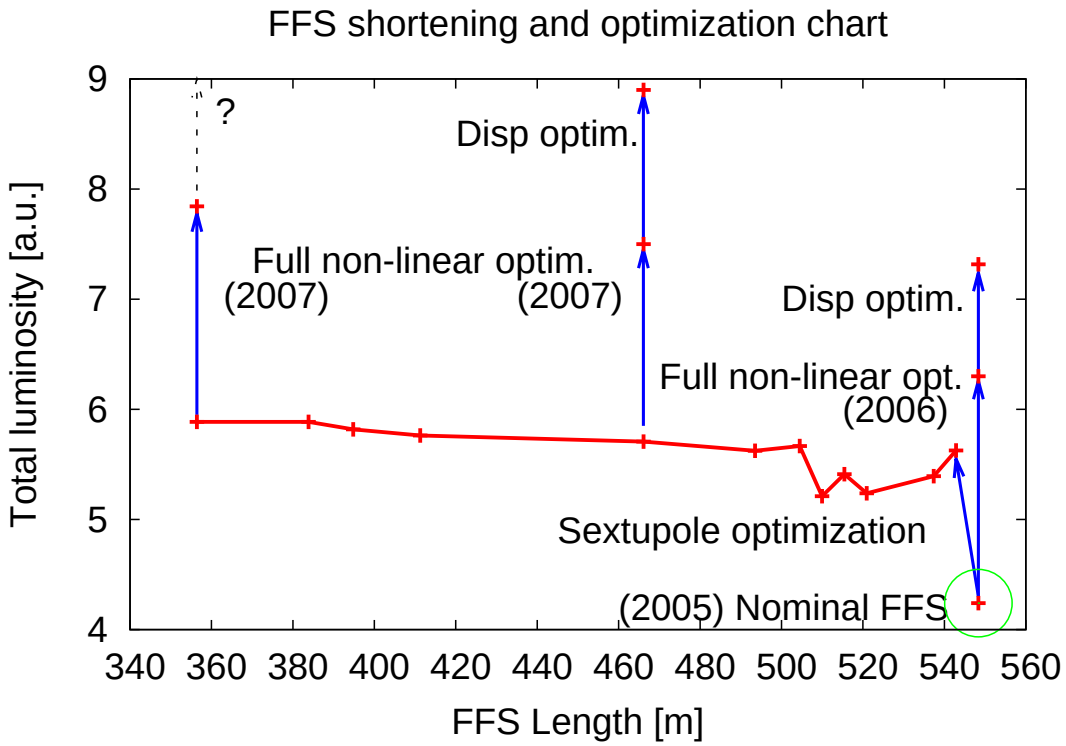

Figure 1: Chart of the optimization of the CLIC Final Focus System showing total luminosity versus the length of the FFS. The starting point is the nominal configuration in 2005. The first optimizations are sextupole and full non-linear. Only after a full non-linear optimization the dispersion is optimized too. After the first sextupole optimization the FFS length starts being reduced (red line) without substantial gain in luminosity. Further optimizations on top of length reductions prove successful. Dispersion optimization was not computed for the shortest system.

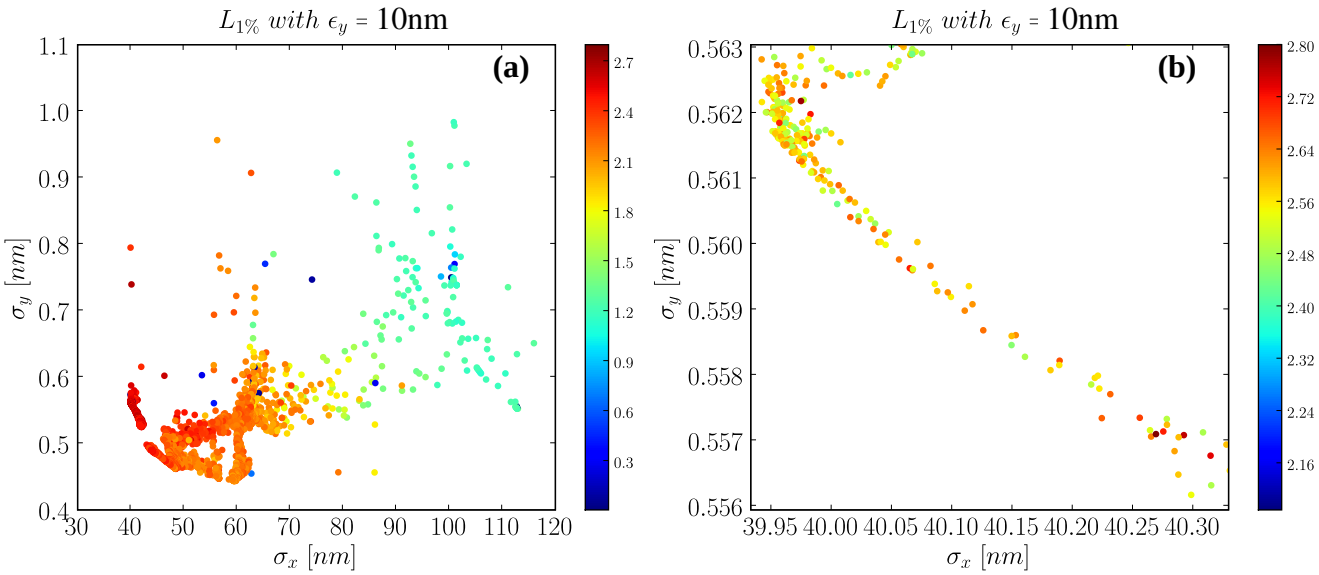

Figure 2: Peak luminosity per bunch crossing taking into account synchrotron radiation effects versus horizontal and vertical beam sizes. Peak luminosity is in arbitrary units and has an uncertainty of 5%. (a) shows all stages of the optimization. (b) shows a zoom containing the maximum peak luminosity. Beam sizes are computed without taking into account synchrotron radiation.

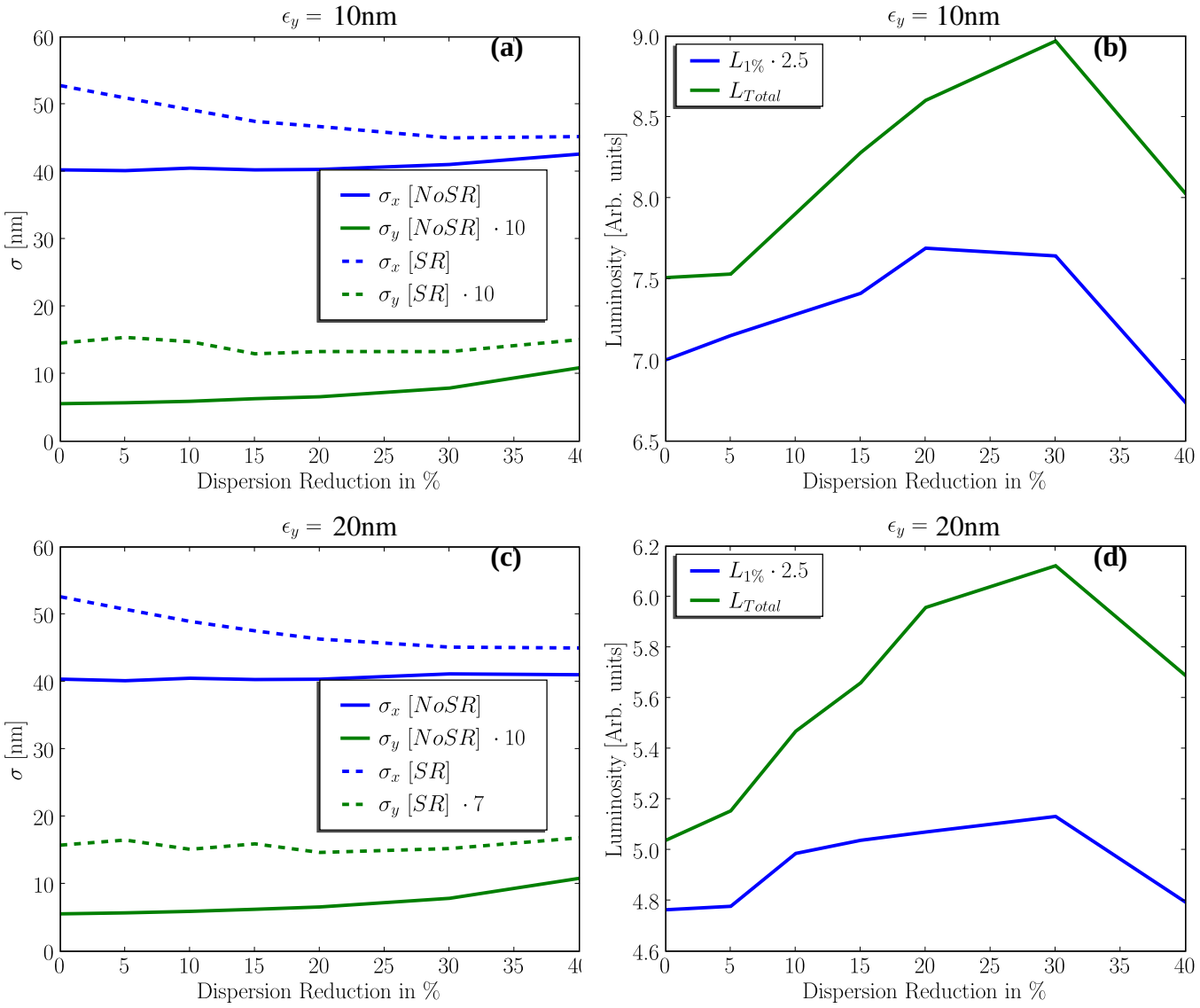

Figure 3: Plots on the left,(a) and (c), show the beam size versus dispersion reduction for the two vertical emittances. Plots on the right, (b) and (d), show the total and peak luminosities versus dispersion reduction. The top plots have a vertical emittance of $0.01\mu m$ while the bottom plots have $0.02\mu m$.

$\epsilon_y = 20$nm, respectively. The horizontal beam size (considering radiation) reduces significantly with lower dispersion. This has a direct impact on the luminosities shown in Fig 3(b) and (d), with maxima at about 30% dispersion reduction, both for $\epsilon_y = 10$nm and $\epsilon_y = 20$nm. Table 1 summarizes all the numerical values of all these plots.

2.1 The longer bunch

Next we investigate the effect of increasing the bunch length from 0.35μm to 0.44μm. The beam sizes and luminosities are shown in Fig. 4 and summarized in table 1. Beam sizes with and without synchrotron radiation and total luminosities behave similarly to those for the shorter bunch length shown above. However peak luminosity shows a totally different dependence on dispersion. For the vertical emittance of $0.02\mu m$ there is no longer a clear peak luminosity maximum, while the total luminosity still has its maximum at about 30% dispersion reduction.

We believe that the saturation of the peak luminosity is due to the increase of beamstrahlung for the longer bunch. The mean beamstrahlung parameter is given in [10] as

$$\Upsilon_{mean} = \frac{5}{6}\frac{N r_e^2 \gamma}{\alpha \sigma_s (\sigma_x + \sigma_y)} \tag{1}$$

and the number of emitted photons is given by

$$n_\gamma = \frac{5}{2}\frac{\alpha^2 \sigma_s}{r_e \gamma}\frac{\Upsilon}{\sqrt{1+\Upsilon^{2/3}}}\,. \tag{2}$$

Using the above equations and that $\Upsilon >> 1$ in the CLIC regime,

$$n_\gamma \propto \frac{\sigma_s^{1/3}}{\sigma_x^{2/3}} \tag{3}$$

Therefore longer σ_s implies more Bremsstrahlung photons. These photon emissions reduce the energy of the particle directly affecting the luminosity at the energy peak but not the total luminosity. Reducing the horizontal spot size also increases the number of photons and this explains why the dispersion optimization does not improve peak luminosity but total luminosity only. We conclude that with these parameters the peak luminosity has been saturated and further reductions of transverse sigmas could enhance total luminosity but not peak luminosity.

3 Performance of the new BDS

So far we have only considered the last part of beam line, the FFS. In this section we compute the performance of the new BDS and compare it to previous designs.

Right at the BDS entrance there is a section that has been recently added: the diagnostics section, Fig. 5. The goals of the diagnostics section are to compensate the transverse coupling errors and to measure emittances and beam energy. The peaks of the vertical β_y have been chosen so that the vertical beam size is 1μm for $\epsilon_y = 20$nm. Present laser wire technology can measure this beam size with a 10% resolution [11].

After the diagnostics section comes the collimation section that has not been modified for the new CLIC parameters yet, although the survival of the beryllium collimators is at risk after having doubled the CLIC number of bunches. The optics and layout of the new BDS is shown in Fig. 6, with at total length of 2750m that could be reduced by 100m if the first 100m were filled with accelerating cavities.

Presently there are three BDS designs with different L*. The original one with 4.3m, the not fully optimized one with L*=2.8m and the latest one with 3.5m L*. The peak luminosities obtained from simulations of these three designs are shown in Fig. 8. For these simulations the latest beam parameters have been used: ϵ_y =20nm and $\sigma_s = 44\mu$m. The shortest FFS shows the worst performance only due to the fact that it was not fully optimized. The other two designs show a very similar performance. This observation is consistent with the above mentioned saturation of the peak luminosity while optimizing the FFS dispersion.

To verify that we have indeed improved the chromatic aberrations by reducing the L* we compare the energy bandwidths of the systems in terms of IP spot sizes and luminosity. Figure 9 shows these bandwidths for the old 4.3m L* and the new 3.5m L* systems. The new shorter FFS has a larger bandwidth for the horizontal IP spot size. It shows a similar effective bandwidth for the vertical IP spot size but left-to-right inverted. Most importantly the bandwidth for the peak luminosity is larger for the shorter system. On the plots an extra curve is shown to which we will refer below.

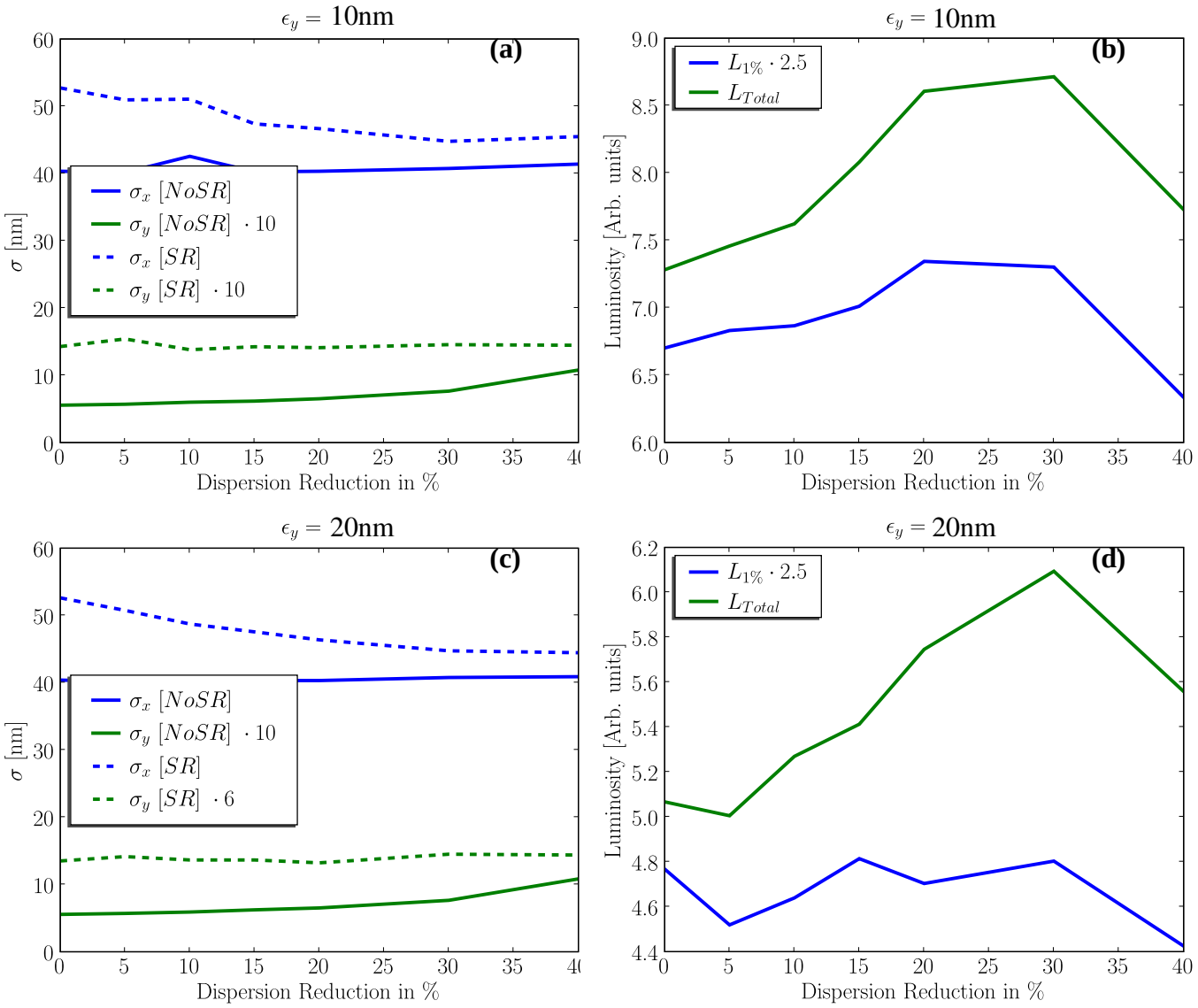

Figure 4: Plots for $\sigma_z = 44\mu$m. On the left,(a) and (c), show the beam size versus dispersion reduction for the two vertical emittances. Plots on the right, (b) and (d), show the total and peak luminosities versus dispersion reduction. The top plots have a vertical emittance of $0.01\mu m$ while the bottom plots have $0.02\mu m$.

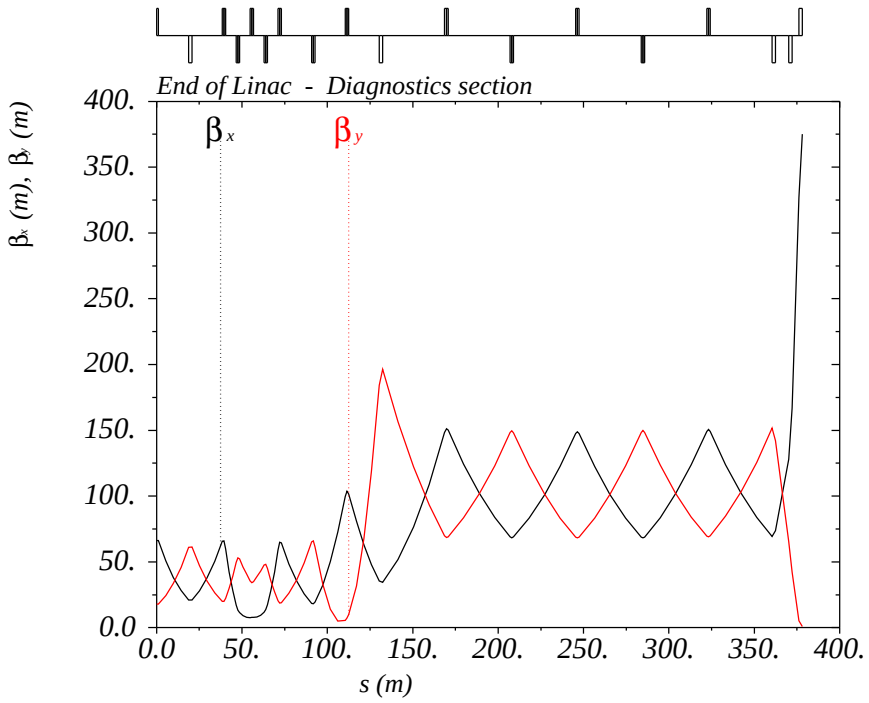

Figure 5: Layout and optics of the diagnostics CLIC section. The peaks of the vertical beta function correspond to 1μm beam size for $\epsilon_y = 20$nm.

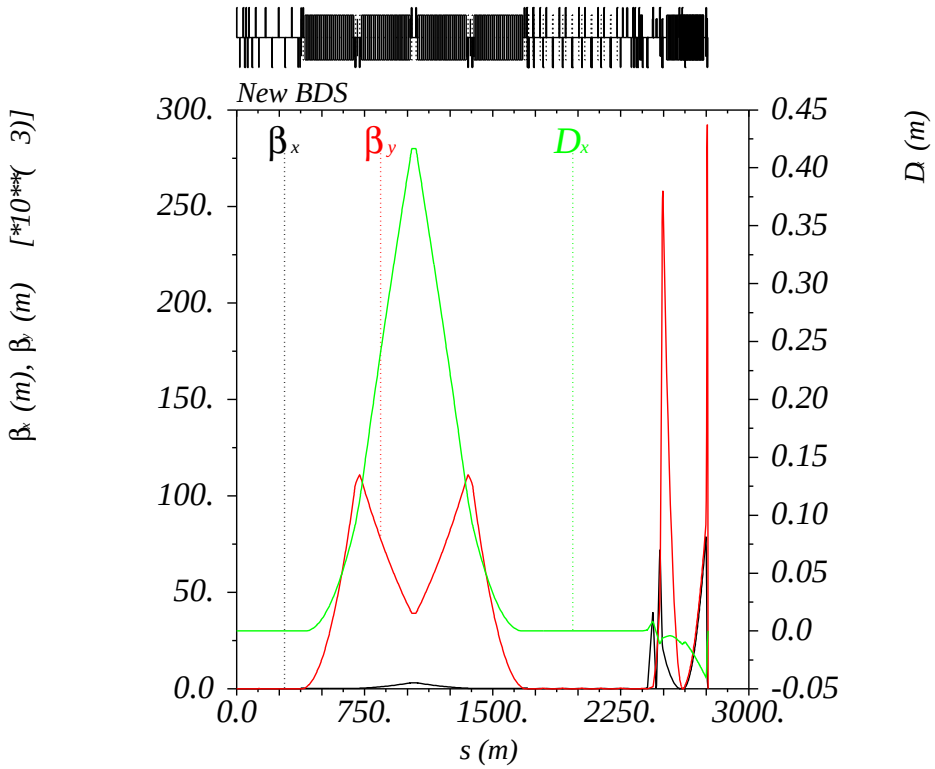

Figure 6: Layout and optics of the full BDS with L* =3.5m.

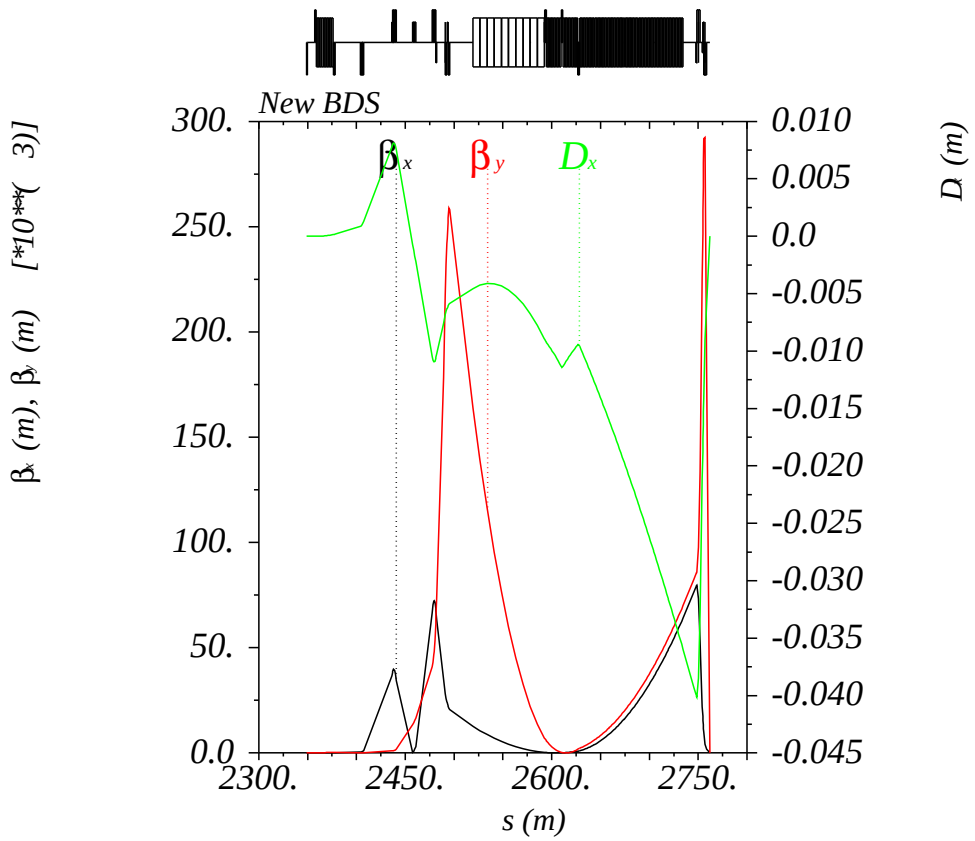

Figure 7: Layout and optics of the FFS with L^* =3.5m.

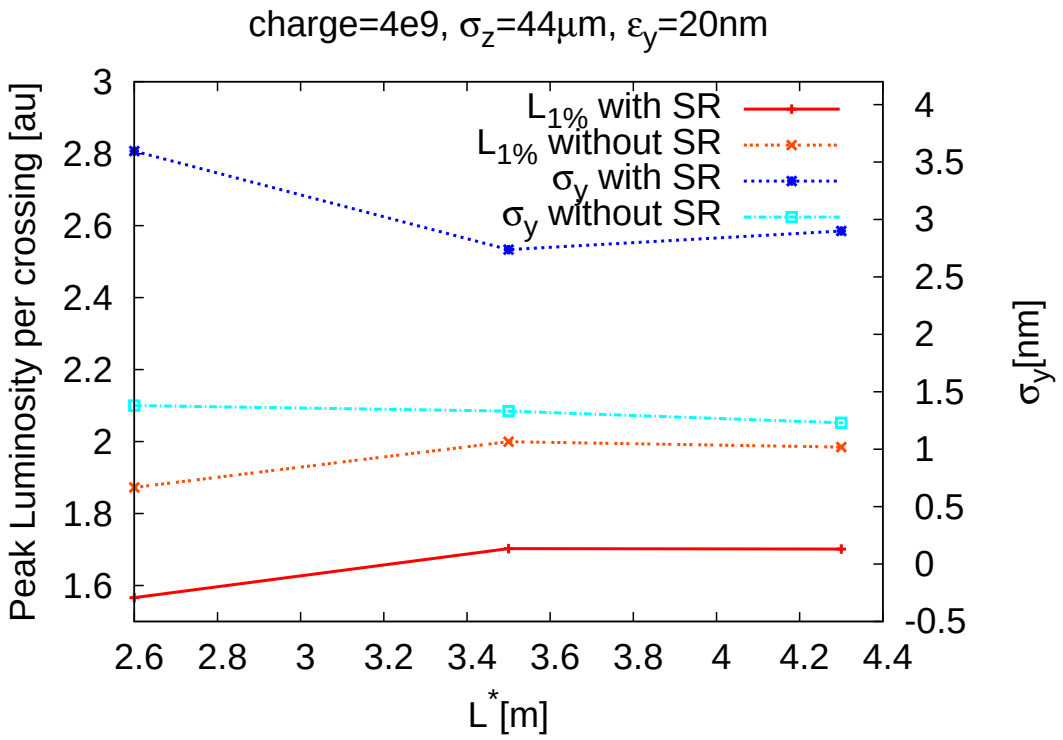

Figure 8: Peak luminosity for the three BDS designs versus L^*. Note that the design with L^*=2.8m was not fully optimized.

Since the final doublet is different for the different FFS designs it is interesting to evaluate and compare the Oide effect [12]. To this end we have tracked with and without synchrotron radiation only through the final doublet until the IP and computed the final beam rms spot sizes. Figure 10 shows the increase in the vertical spot size caused by considering synchrotron radiation in the final doublet. It is clear that the 3.5m L^* option is the most affected by the Oide effect. A first attempt to reduce the Oide effect for this option has been exercised by increasing the length of the final doublet magnets by 0.1m, corresponding to a relative increase of about 7%. After a full optimization of this new FFS the Oide effect has decreased by a factor of two (even below the other systems). A much more modest increase in the peak luminosity by about 5% has been found since it is well known that the Oide effect affects mostly the tails of the bunch, which do not contribute much to the luminosity. However the bandwidth of this new system with a radiation optimized doublet has also been computed and it has been found to be slightly worse than the previous 3.5m L^* FFS, see Fig. 9.

4 Summary and conclusion

A full optimization of the CLIC BDS has been presented for the new $L^* = 3.5$m and new beam parameters. During the optimization processes it has been observed that further reductions of the horizontal spot size do not translate into a peak luminosity gain for the new parameters, contrary to the trend for the old parameters (shorter bunch and smaller vertical emittance). We conclude that the new parameters have caused a saturation of the peak luminosity due to the enhanced Beamstrahlung at the IP. Basically the machine performance is limited by the beam-beam interaction and not by the machine optics.

The Oide effect has been investigated, observing that it has been enhanced for the new $L^* = 3.5$m FFS. A minimization of this effect has been achieved by a small increase on the length of the final

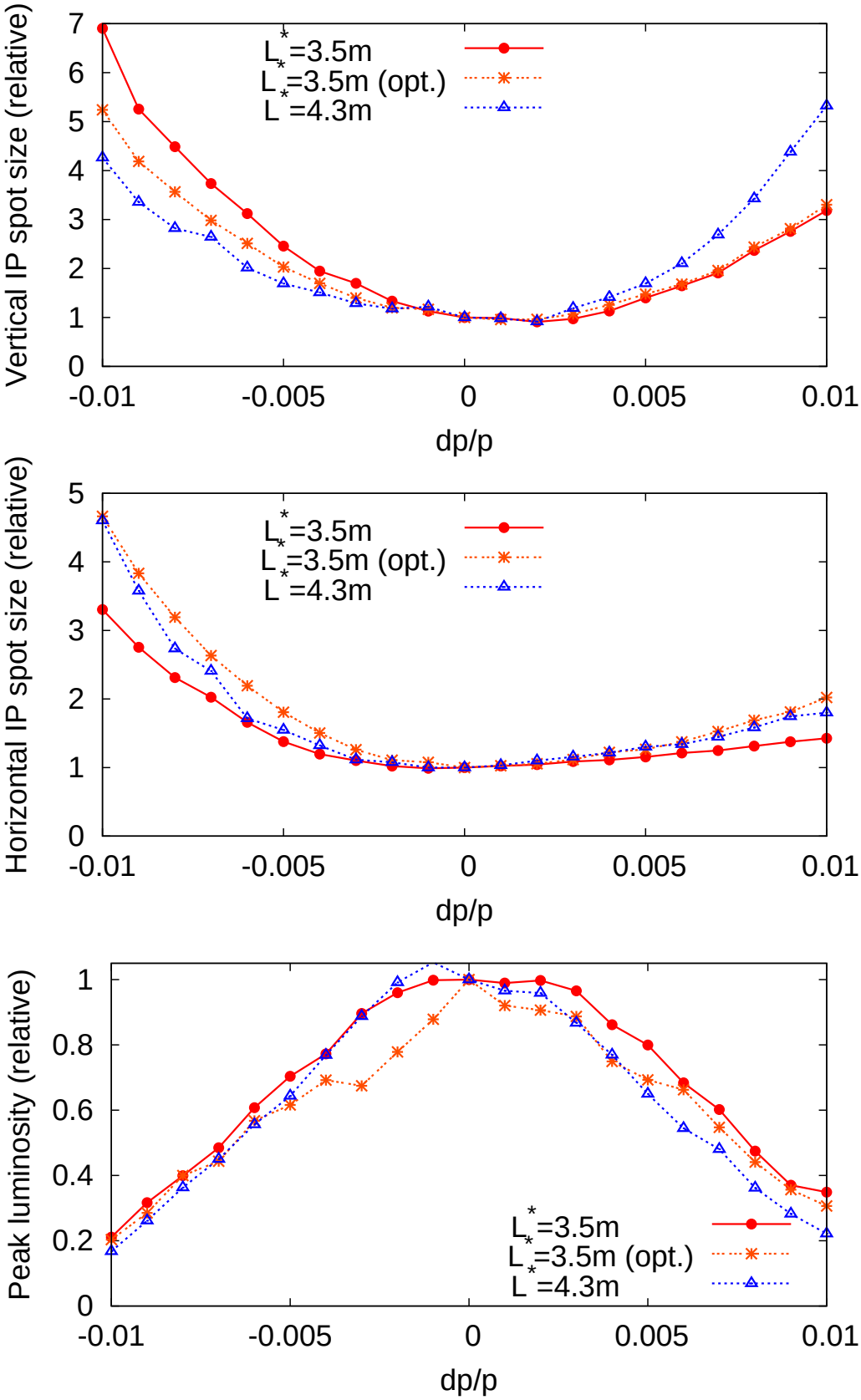

Figure 9: Bandwidth plots for three different FFS: the old 4.3m L^*, the new 3.5m L^* and another radiation optimized 3.5m L^* system with the label (opt). The latter corresponds to an FFS with 7% longer final doublet in order to reduce the Oide effect. In descending order the plots show vertical spot size, horizontal spot size and peak luminosity versus relative momentum deviation. The shorter system exhibits a larger peak luminosity bandwidth.

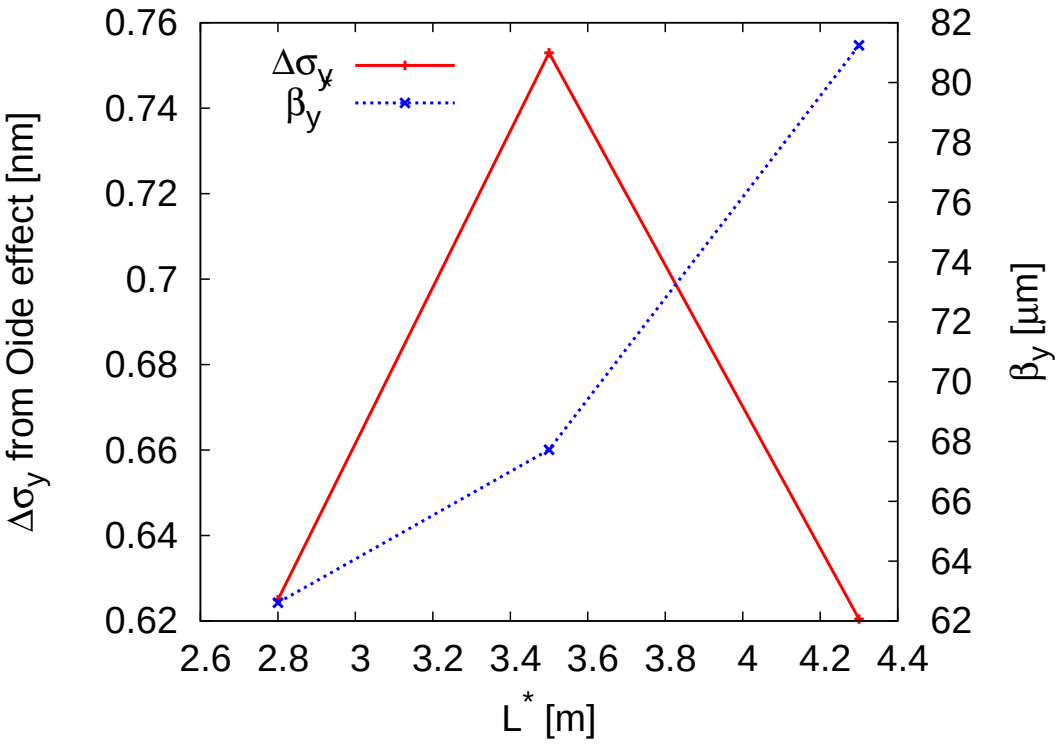

Figure 10: Increase in the IP vertical beam size caused by considering synchrotron radiation in the final doublet versus L*. All cases are computed for a vertical normalized emittance of ϵ_y=20nm

doublet. The Oide effect has been reduced by a factor two but peak luminosity showed only a moderate increase in the percent level, as expected since the Oide effect does not affect the core of the beam but the tails. However this change in the optics of the system has turned out into a slight reduction of bandwidth.

In conclusion three different FFS designs exist with similar performance in terms of peak luminosity and with different features:

- **L*=4.3m**, easiest detector integration due to the longer L*.
- **L*=3.5m**, largest energy bandwidth.
- **L*=3.5m, radiation optimized**, lowest synchrotron radiation at the final doublet.

All these lattices are stored in the CLIC lattice repository [13]. we choose the **L*=3.5m** option as the CLIC BDS baseline design since it has a slightly larger bandwidth and needs a shorter tunnel.

Acknowledgments

Thanks to H. Braun and D. Schulte for motivating this study and their fruitful suggestions.

References

[1] R. Tomás, "Non-linear Optimization of Beam Lines", Phys. Rev. ST Accel. Beams **9**, 081001 (2006).

$\epsilon_y = 0.01\mu$m, $\sigma_z = 35\mu$m for the FFS

Disp. Red. [%]	L_{tot} $[au]$	$L_{1\%}$ $[au]$	σ_x NoSR $[nm]$	σ_y NoSR $[nm]$	σ_x SR $[nm]$	σ_y SR $[nm]$
0	7.51	2.80	40.26	0.557	52.77	1.45
5	7.53	2.86	40.15	0.570	50.94	1.54
10	7.90	2.91	40.52	0.592	49.19	1.47
15	8.28	2.96	40.26	0.631	47.46	1.29
20	8.60	3.08	40.33	0.659	46.69	1.33
30	8.97	3.06	41.06	0.788	45.01	1.33
40	8.03	2.69	42.60	1.089	45.20	1.50

$\epsilon_y = 0.02\mu$m, $\sigma_z = 35\mu$m for the FFS

Disp. Red. [%]	L_{tot} $[au]$	$L_{1\%}$ $[au]$	σ_x NoSR $[nm]$	σ_y NoSR $[nm]$	σ_x SR $[nm]$	σ_y SR $[nm]$
0	5.03	1.90	40.38	0.555	52.61	2.25
5	5.15	1.91	40.15	0.570	50.75	2.35
10	5.46	1.99	40.52	0.592	48.95	2.16
15	5.66	2.01	40.32	0.623	47.55	2.27
20	5.95	2.02	40.37	0.658	46.33	2.09
30	6.12	2.05	41.16	0.786	45.13	2.17
40	5.68	1.91	41.04	1.082	45.01	2.40

$\epsilon_y = 0.01\mu$m, $\sigma_z = 44\mu$m for the FFS

Disp. Red. [%]	L_{tot} $[au]$	$L_{1\%}$ $[au]$	σ_x NoSR $[nm]$	σ_y NoSR $[nm]$	σ_x SR $[nm]$	σ_y SR $[nm]$
0	7.28	2.68	40.33	0.556	52.72	1.42
5	7.45	2.73	40.15	0.570	50.94	1.54
10	7.62	2.74	42.55	0.600	51.05	1.38
15	8.08	2.80	40.25	0.616	47.38	1.42
20	8.60	2.93	40.33	0.651	46.67	1.41
30	8.71	2.92	40.75	0.765	44.78	1.45
40	7.72	2.53	41.40	1.078	45.48	1.44

$\epsilon_y = 0.02\mu$m, $\sigma_z = 44\mu$m for the FFS

Disp. Red. [%]	L_{tot} $[au]$	$L_{1\%}$ $[au]$	σ_x NoSR $[nm]$	σ_y NoSR $[nm]$	σ_x SR $[nm]$	σ_y SR $[nm]$
0	5.06	1.90	40.38	0.555	52.61	2.25
5	5.00	1.80	40.15	0.570	50.75	2.35
10	5.26	1.85	40.24	0.590	48.73	2.27
15	5.41	1.92	40.31	0.623	47.55	2.27
20	5.74	1.88	40.32	0.651	46.37	2.20
30	6.09	1.92	40.77	0.765	44.74	2.41
40	5.55	1.77	40.89	1.083	44.45	2.39

Table 1: FFS summary tables. Luminosities and IP beam sizes for the different beam parameters and dispersion reductions.

[2] J.A. Nelder and R. Mead, Computer Journal, 1965, vol **7**, pp 308-313.

[3] R. Tomás , "Nonlinear optimization of beam lines", CERN-OPEN-2006-023 ; CLIC-Note-659 (2006).

[4] P. R. Jarnhus, R. Tomás, "Optimization of the CLIC Final Focus dispersion without using extra multipolar components" CERN AB-Note-2007-006.

[5] R. Tomás, "MAPCLASS: a code to optimize high order aberrations" CERN AB-Note-2006-017 (ABP).

[6] H. Grote and F. Schmidt, "MAD-X - An Upgrade from MAD8", CERN-AB-2003-024, ABP.

[7] E. Forest, F. Schmidt and E. McIntosh, "Introduction to the Polymorphic Tracking Code", KEK Report 2002-3.

[8] R. Tomás, M. Giovannozzi and R. de Maria, "IR multipolar correction for the LHC upgrade", in proceedings of IR'07 CARE-HHH-APD, Frascati 2007.

[9] D. Schulte, "Beam-Beam Simulations with GUINEA-PIG", ICAP98, Monterey, CA., USA (1998).

[10] L. Z. Rivkin, "Beamstrahlung and Disruption" CERN 95-06 vol. 2, prepared for CERN Accelerator School: Course on Advanced Accelerator Physics (CAS), Rhodes, Greece (1993).

[11] S. T. Boogert et al, "A LASER-WIRE SYSTEM AT THE ATF EXTRACTION LINE", EPAC 2006.

[12] K. Oide, "Synchrotron-Radiation Limit on the Focusing of Electron Beams", Phys. Rev. Lett. **61**, 1713 - 1715 (1988).

[13] CLIC lattice repository: http://clicr.web.cern.ch/CLICr/